

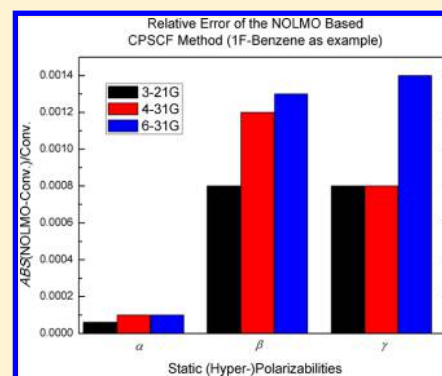
Coupled-Perturbed SCF Approach for Calculating Static Polarizabilities and Hyperpolarizabilities with Nonorthogonal Localized Molecular Orbitals

Shaopeng Li,[†] Linping Hu,[†] Liang Peng,[†] Weitao Yang,^{†,‡} and Feng Long Gu^{*,†}

[†]Key Laboratory of Theoretical Chemistry of Environment, Ministry of Education, School of Chemistry & Environment, South China Normal University, Guangzhou 510006, China

[‡]Department of Chemistry and Physics, Duke University, Box 90346, Durham, North Carolina 27708-0346, United States

ABSTRACT: Coupled-perturbed self-consistent-field (CPSCF) approach has been broadly used for polarizabilities and hyperpolarizabilities computation. To extend this application to large systems, we have reformulated the CPSCF equations with nonorthogonal localized molecular orbitals (NOLMOs). NOLMOs are the most localized representation of electronic degrees of freedom. Methods based on NOLMOs are potentially ideal for investigating large systems. In atomic orbital representation, with a static external electric field added, the wave function and SCF operator of unperturbed NOLMO-SCF wave function/orbitals are expanded to different orders of perturbations. We have derived the corresponding equations up to the third order, which are significantly different from those of a conventional CPSCF method because of the release of the orthogonal restrictions on MOs. The solution to these equations has been implemented. Several chemical systems are used to verify our method. This work represents the first step toward efficient calculations of molecular response and excitation properties with NOLMOs.



I. INTRODUCTION

Coupled-perturbed self-consistent-field (CPSCF) method has been widely used to investigate molecular properties of molecules responding to an external electric field. The response is evaluated via calculations of polarizabilities and hyperpolarizabilities. Polarizabilities and hyperpolarizabilities provide important characterization of materials for efficiency as optical fibers, optical frequency converters and electrooptic modulators, and thin-film transistor displays.^{1–6} To investigate these properties, accurate calculations are required, as calculations of such properties are routinely carried out with ab initio quantum-chemical methods.^{7–14} Among these methods, the framework proposed by Karna and Dupuis⁹ has been widely used.

Polarizabilities and hyperpolarizabilities can be obtained by an iterative solution of the CPSCF equations. These SCF theories include the Hartree–Fock (HF), Kohn–Sham density functional theory (KS-DFT), and hybrid HF-DFT models. In these approaches, an external electric field is added to the effective Fock/Kohn–Sham Hamiltonian. This perturbation gives rise to deviations of the wave function from the unperturbed solutions. Based on perturbation theory, the wave function and the Fock/KS operators are expanded in various orders of the electric field. Then the equations of each order are obtained. Solving these equations leads to the first and higher order density matrices, which are necessary for calculating polarizabilities and hyperpolarizabilities. The equations used in CPDFT are similar to those used in CPHF.¹⁵ The main difference is that the HF exchange potential in CPHF

method is replaced by an (approximate) exchange–correlation (xc) potential in CPDFT method.

However, CPSCF methods have been developed traditionally with canonical molecular orbitals (CMOs) basis, which extend over the entire molecular system. In these methods, an atomic orbital–molecular orbital (AO–MO) integral transformation entails an overall $O(N^5)$ (N is the number of basis functions) computational scaling. An alternative direct contraction of the two-electron integrals in the AO basis is straightforward that reduces the scaling to $O(N^3)$ for each perturbation of the density matrix.¹⁶ This has been the main bottleneck of calculating the polarizabilities and hyperpolarizabilities for large systems. Indeed, linear-scaling, $O(N)$, methods are desirable.

Because linear-scaling methods can deal with large systems without losing significant accuracy, developing linear-scaling methods remains active.^{17–19} In general, to achieve linear scaling, existence of solutions to molecular orbitals or density matrices that are localized in real space should be satisfied. Thus, there are two main categories of approaches to linear scaling, either with density matrix or with localized molecular orbitals (LMOs). To reduce the scaling of CPSCF theory to linear, a density matrix based method will reformulate all MO based quantities fully in the AO basis. Then in combination with some other techniques, e.g., the fast multipole method^{20,21} and the use of efficient sparse matrix scheme,²² the overall

Received: October 6, 2014

Published: February 5, 2015

scaling can be reduced to linear. In contrast, an LMO based method will localize the CMOs first. Then based on the LMOs, certain cutoff²³ technology that avoids calculations of a large part of the density matrix generation during SCF processes can be employed to reduce the computational cost significantly. Then also with the fast multipole method the overall scaling can be reduced to linear. The density matrix based linear-scaling methods have been reviewed recently by Kussmann et al.¹⁷ We focus on the LMO based methods in this work.

Compared with CMOs, LMOs can achieve more localized orbital distributions in a limited spatial region, which is important for reducing the computational effort in the linear-scaling algorithms. There are two types of LMOs: one is the extensively investigated orthogonal LMOs (OLMOs), and the other is the nonorthogonal LMOs (NOLMOs). As the OLMOs generation from CMOs has been largely explored,^{24–29} many (nearly) linear-scaling methods have been developed with this basis, e.g., the local space approximation given by Kirtman et al.^{30,31} and the elongation method proposed by Imamura et al.^{32–34} These methods have been widely used on investigating large systems, e.g., nanomaterials or biological systems.^{35–37} Moreover, another reason for using OLMOs in these methods is that the orthogonal properties among the LMOs keep the equations of the wave function and Fock/KS operators almost unchanged. This results in a relatively convenient implementation of computer code. However, the main problem with OLMOs is that they possess long-range nonlocalized tails, or delocalization tails,³⁸ outside the localization center which reduces computational efficiency and complicates the transferability of descriptions of LMOs from one system to another.

In contrast, NOLMOs can achieve more compact/localized LMOs than OLMOs.³⁹ The reason for this improvement is from the release of orthogonal constraints of the MOs. As a result, the long-range tails of the OLMOs are removed and more localized distributions of electrons in space are obtained. Moreover, NOLMO based methods can lead to significantly more accurate results than OLMO based methods with the same local regions used.⁴⁰ This is made possible because NOLMO based methods can generate more accurate density matrix than OLMO based methods if the same cutoff threshold is used in both methods. However, NOLMO based methods require a significant modification to the related equations because the orthogonal restriction of the MOs is removed. Nevertheless, owing to the advantages of the NOLMO basis, more and more attention has been attracted to the development of NOLMO based methods.^{18,40,41} With efficient NOLMO construction algorithms,⁴² a few linear-scaling NOLMO based methods have been developed to explore the ground and excited states of molecules: the NOLMO based HF and DFT methods for ground state calculations,^{18,40} the NOLMO based time-dependent density functional theory (TDDFT) method with self-consistent charge density functional tight-binding (SCC-DFTB),⁴¹ and quantum Monte Carlo (QMC) method.⁴³

Although a few density matrix based linear-scaling methods have been developed for calculating the polarizabilities and hyperpolarizabilities of molecules,^{44,45} to our knowledge, applying NOLMOs to CPSCF method has not yet been explored. Since NOLMO basis has many advantages compared with the OLMOs, a NOLMO based CPSCF method would be potentially a linear-scaling method that allows us to investigate large systems. We present in this work an NOLMO based

CPSCF method for calculating static polarizabilities and hyperpolarizabilities. In our method, a static external electric field is added to an unperturbed reference, which is obtained from a NOLMO-SCF ground state calculation. The perturbation expands the corresponding wave function and the SCF operators into different orders. Because of the release of orthogonal constraints of the MOs, the equations of these orders in our method will be very different from those of a CMO based method. Solving these equations will lead to density matrices corresponding to the different orders. With these density matrices, we can obtain polarizabilities and hyperpolarizabilities of molecules. We have implemented these equations into computer code. And to verify our method, standard GAMESS CPSCF calculations⁴⁶ have been used as a benchmark. Water dimer, naphthalene, 1-fluorobenzene, and $\text{CH}_2(\text{CH})_8\text{CH}_2$ have been used as test systems. The results show that NOLMO-CPSCF has a good accuracy. However, at this stage, we have introduced neither cutoff scheme nor the use of sparse matrix in our method. These technologies will be applied in our method in future work. Future work will also include frequency-dependent wave functions into the equations for NOLMO based TDSCF method.

This work is organized as follows: Section II gives the detailed derivation of the NOLMO based CPSCF formulas for each order of the static perturbations, while section III presents some key steps in the computer implementation. Calculations of the static polarizabilities and static hyperpolarizabilities of the test systems are carried out by both of our code and the standard GAMESS CPSCF code. The results are listed in section IV. Section V gives a short discussion. Finally, a conclusion has been drawn in section VI.

II. NOLMO-CPSCF EQUATIONS

1. Review of the Unperturbed Ground State NOLMO-SCF Approach. We first review the equations that describe the NOLMO of the unperturbed ground state. The ground state energy, $W(\hat{\rho})$, of a system with N electrons in a spin-compensated situation is a function of the one-electron density matrix, $\langle \mathbf{r}_1 | \hat{\rho} | \mathbf{r}_2 \rangle = \rho(\mathbf{r}_1, \mathbf{r}_2)$. This energy, for Hartree-Fock and Kohn-Sham density functional theories, is defined as

$$W[\hat{\rho}] = \text{Tr}[t + v_{\text{ext}}]\hat{\rho} + W_j[\hat{\rho}] + W_{\text{xc}}[\hat{\rho}] \quad (1)$$

where t is the one-electron kinetic energy operator, v_{ext} is the nuclear-electron interaction operator, $W_j[\hat{\rho}] = (1/2) \int (\rho(\mathbf{r}_1)\rho(\mathbf{r}_2)/(|\mathbf{r}_1 - \mathbf{r}_2|)) \, d\mathbf{r}_1 \, d\mathbf{r}_2$ is the classical electron-electron Coulomb interaction energy, and $W_{\text{xc}}[\hat{\rho}]$ is the exchange-correlation energy. In DFT, $W_{\text{xc}}[\hat{\rho}]$ depends on the chosen functional, while, in HF theory, $W_{\text{xc}}[\hat{\rho}]$ is the exchange energy functional: $W_{\text{xc}}[\hat{\rho}] = (1/4) \int (|\rho(\mathbf{r}_1, \mathbf{r}_2)|^2 / (|\mathbf{r}_1 - \mathbf{r}_2|)) \, d\mathbf{r}_1 \, d\mathbf{r}_2$ for restricted description of closed-shell systems. The NOLMO-SCF ground state energy of an N -electron closed-shell system is obtained via minimum principle as

$$W^0(N) = \min W[\hat{\rho}^0] \quad (2)$$

where the superscript, 0, indicates the ground state unperturbed energy. The density operator, $\hat{\rho}$, must satisfy the conditions of Hermitian requirement ($\hat{\rho} = \hat{\rho}^\dagger$), idempotency ($\hat{\rho}^2 = \hat{\rho}$), and normalization ($\text{Tr}(\hat{\rho}) = N$). It can be generated from a set of not necessarily orthonormal but linear-independent orbitals, $\{\psi_i^0\}$, as

$$\hat{\rho}^0 = 2 \sum_{i,j}^{N/2} |\psi_i^0\rangle \langle \mathbf{S}^{(0)-1} \rangle_{ij} \langle \psi_j^0| \quad (3)$$

where $\{\psi_i^0\}$ are obtained via linear combination of AOs, $\psi_i^0 = \sum_{\mu}^{\text{AO}} C_{\mu i}^0 \chi_{\mu}$ of which $C_{\mu i}$ are the orbital coefficients and $\mathbf{S}^{(0)-1}$ is the unperturbed inverse of the unperturbed overlap matrix \mathbf{S}^0 :

$$\mathbf{S}_{ij}^0 = \langle \psi_i^0 | \psi_j^0 \rangle = \sum_{\mu,\nu} C_{\mu i}^0 \langle \chi_{\mu} | \chi_{\nu} \rangle C_{\nu j}^0 = \sum_{\mu,\nu} C_{\mu i}^0 s_{\mu\nu} C_{\nu j}^0 \quad (4)$$

In order to generate the inverse matrix in a linear-scaling manner, using the energy minimum principle proved by Yang,⁴⁷ a truncated approximation to the matrix $\mathbf{S}^{(0)-1}$ can be obtained with $O(N)$ operations via the relation of $\text{Tr}[B^{\text{pos}} \mathbf{S}^{(0)-1}] = \min_{X=X^\dagger} \text{Tr}[B^{\text{pos}}(2X - X\mathbf{S}X)]$ with B^{pos} as any positive definite matrix. Thus, we can express $\mathbf{S}^{(0)-1}$ as

$$\mathbf{S}^{(0)-1} = 2\mathbf{X} - \mathbf{X}\mathbf{S}^0\mathbf{X} \quad (5)$$

where the matrix \mathbf{X} is constrained to be Hermitian treated as an auxiliary matrix that becomes $\mathbf{S}^{(0)-1}$ when W is at its minimum. With eq 3 and eq 5, eq 2 leads to the variational principle in terms of NOLMO,⁴⁷

$$W^0(N) = \min_{\{\psi_i^0\}} \min_{X=X^\dagger} \Omega[(2X - X\mathbf{S}^0X), \{\psi_i^0\}] + \eta N \quad (6)$$

where Ω is defined as

$$\Omega[\mathbf{S}^{(0)-1}, \{\psi_i^0\}] = W[\hat{\rho}^0] - \eta \text{Tr}(\hat{\rho}^0) \quad (7)$$

and η is a parameter that should be larger than the largest eigenvalue of the canonical solution. It is always chosen to be a constant for a desired energy minimization process. From eq 3, the density matrix of the NOLMO-SCF method is expanded as

$$\begin{aligned} \langle \mathbf{r}_1 | \hat{\rho}^0 | \mathbf{r}_2 \rangle &= 2 \sum_{ij} \sum_{\mu\nu} \langle \mathbf{r}_1 | \chi_{\mu} \rangle C_{\mu i}^0 S_{ij}^{(0)-1} C_{\nu j}^0 \langle \chi_{\nu} | \mathbf{r}_2 \rangle \\ &= \sum_{\mu\nu} \langle \mathbf{r}_1 | \chi_{\mu} \rangle D_{\mu\nu}^0 \langle \chi_{\nu} | \mathbf{r}_2 \rangle \end{aligned} \quad (8)$$

with the ground state unperturbed density matrix elements defined as

$$D_{\mu\nu}^0 = 2 \sum_{i,j} C_{\mu i}^0 S_{ij}^{(0)-1} C_{\nu j}^{(0)*} \quad (9)$$

In matrix notation, eq 9 is written as

$$\mathbf{D}^0 = 2\mathbf{C}^0 \mathbf{S}^{(0)-1} \mathbf{C}^{0\dagger} \quad (10)$$

The derivative of eq 7 with respect to the density matrix will give us the Fock/Kohn–Sham operator as

$$\frac{\partial \Omega}{\partial D_{\mu\nu}^0} = f_{\nu\mu}^0 - \eta s_{\nu\mu} = F_{\nu\mu}^0 \quad (11)$$

The general expression of this operator is written as

$$F_{\mu\nu}^0 = v_{\mu\nu} + V_{\mu\nu}^{(0)J} + V_{\mu\nu}^{(0)xc} \quad (12)$$

where $v_{\mu\nu}$ is the one-electron integral matrix elements,

$$v_{\mu\nu} = \left\langle \chi_{\mu} \left| -\frac{1}{2} \nabla_i^2 - \sum_k^{\text{nuclei}} \frac{Z_k}{r_k} \right| \chi_{\nu} \right\rangle \quad (13)$$

and $V_{\mu\nu}^J$ is the Coulomb repulsion, $V_{\mu\nu}^{xc}$ indicates the exchange potential in the HF theory or (approximate) exchange-

correlation potential in Kohn–Sham DFT. From eq 12, the ground state unperturbed Hamiltonian matrix is generated as

$$\mathbf{H}^0 = \mathbf{C}^{0\dagger} \mathbf{F}^0 \mathbf{C}^0 \quad (14)$$

2. NOLMO-CPSCF Equations. From a NOLMO-SCF reference described earlier, with a static external electric field, \vec{E} , added, the dipolar interaction Hamiltonian for perturbation can be written as

$$\mathbf{H}(\vec{E}) = \vec{\mu} \cdot \vec{E} \quad (15)$$

where $\vec{\mu}$ is the dipole moment operator

$$\vec{\mu} = - \sum_i^N (e \cdot \mathbf{r}_i) \quad (16)$$

with e indicating the electronic charge and \mathbf{r}_i denoting the position vector of the i th electron. The electronic part of the Schrödinger equation for the molecule with a static external electric field can thus be written as

$$(\mathbf{H}^0 + \mathbf{H}(\vec{E}))\Psi = W\Psi \quad (17)$$

where W indicates the total energy of the molecule in the static external field. The AOs, $\{\chi_{\mu}\}$, which we choose to expand the NOLMOs, are independent of the external electric field. So we will have

$$s_{\mu\nu} \equiv s_{\mu\nu}^0 = \langle \chi_{\mu} | \chi_{\nu} \rangle \quad (18)$$

Other perturbed matrices can be expanded by applying the static field as a function of the magnitude and direction of the electric field as

$$\mathbf{C}(\vec{E}) = \mathbf{C}^0 + E^a \mathbf{C}^a + (2!)^{-1} E^a E^b \mathbf{C}^{ab} + (3!)^{-1} E^a E^b E^c \mathbf{C}^{abc} + \dots \quad (19)$$

$$\mathbf{F}(\vec{E}) = \mathbf{F}^0 + E^a \mathbf{F}^a + (2!)^{-1} E^a E^b \mathbf{F}^{ab} + (3!)^{-1} E^a E^b E^c \mathbf{F}^{abc} + \dots \quad (20)$$

$$\mathbf{D}(\vec{E}) = \mathbf{D}^0 + E^a \mathbf{D}^a + (2!)^{-1} E^a E^b \mathbf{D}^{ab} + (3!)^{-1} E^a E^b E^c \mathbf{D}^{abc} + \dots \quad (21)$$

The superscripts a , b , and c , etc., in eqs 19–21 denote the direction of the perturbation while their number represents the order of the perturbation; e.g., \mathbf{C}^a ($a \in \{x, y, z\}$) means the first order of the perturbation while \mathbf{C}^{ab} ($a, b \in \{x, y, z\}$) and \mathbf{C}^{abc} ($a, b, c \in \{x, y, z\}$) are the second and third order of the perturbations, respectively. Substituting eq 19 into eq 4, we get the perturbation form of the overlap matrix as

$$\mathbf{S}(\vec{E}) = \mathbf{S}^0 + E^a \mathbf{S}^a + (2!)^{-1} E^a E^b \mathbf{S}^{ab} + (3!)^{-1} E^a E^b E^c \mathbf{S}^{abc} + \dots \quad (22)$$

where \mathbf{S}^0 (eq 4),

$$\mathbf{S}^a = \sum_{(i,j) \in \Lambda_{\text{comb}}^a} \mathbf{C}^{i\dagger} \mathbf{S}^a \mathbf{C}^j \quad (23)$$

$$\mathbf{S}^{ab} = \sum_{(i,j) \in \Lambda_{\text{comb}}^{ab}} \mathbf{C}^{i\dagger} \mathbf{S}^{ab} \mathbf{C}^j \quad (24)$$

$$\mathbf{S}^{abc} = \sum_{(i,j) \in \Lambda_{\text{comb}}^{abc}} \mathbf{C}^{i\dagger} \mathbf{S}^{abc} \mathbf{C}^j \quad (25)$$

are the first order, second order, and third order perturbations, respectively. The Λ_{comb}^x appearing in eqs 23–25 are the combinations of the possible values for the (i, j) pair:

$$\Lambda_{\text{comb}}^a = \{(0, a), (a, 0), (0, 0, a), (0, a, 0), (a, 0, 0), (0, 0, 0, a), (0, 0, a, 0), (0, a, 0, 0), (a, 0, 0, 0)\} \quad (26)$$

$$\Lambda_{\text{comb}}^{ab} = \{(0, ab), (ab, 0), (a, b), (b, a), (0, 0, ab), (0, ab, 0), (ab, 0, 0), (a, b, 0), (a, 0, b), (b, 0, a), (0, 0, a, b), (0, 0, ab, 0), (0, ab, 0, 0), (0, 0, a, b), (0, 0, b, a), (0, a, 0, b), (0, b, 0, a), (a, 0, 0, b), (b, 0, 0, a), (0, a, b, 0), (0, b, a, 0), (a, 0, b, 0), (b, 0, a, 0), (a, b, 0, 0), (b, a, 0, 0)\} \quad (27)$$

$$\Lambda_{\text{comb}}^{abc} = \{(0, abc), (abc, 0), (ab, c), (ac, b), (bc, a), (a, bc), (b, ac), (c, ab), (0, 0, abc), (0, abc, 0), (abc, 0, 0), (ac, b, 0), (bc, a, 0), (ab, 0, c), (ac, 0, b), (bc, 0, a), (0, ab, c), (0, ac, b), (0, bc, a), (a, bc, 0), (b, ac, 0), (c, ab, 0), (a, 0, bc), (b, 0, ac), (c, 0, ab), (a, b, c), (a, c, b), (b, a, c), (b, c, a), (c, a, b), (c, b, a), (0, 0, 0, abc), (0, 0, abc, 0), (0, abc, 0, 0), (abc, 0, 0, 0), (0, 0, a, bc), (0, 0, b, ac), (0, 0, c, ab), (0, 0, ab, c), (0, 0, ac, b), (0, 0, bc, a), (0, a, 0, bc), (0, b, 0, ac), (0, c, 0, ab), (0, ab, 0, c), (0, ac, 0, b), (0, bc, 0, a), (a, 0, 0, bc), (b, 0, 0, ac), (c, 0, 0, ab), (ab, 0, 0, c), (ac, 0, 0, b), (bc, 0, 0, a), (a, 0, bc, 0), (b, 0, ac, 0), (c, 0, ab, 0), (ab, 0, c, 0), (ac, 0, b, 0), (bc, 0, a, 0), (a, bc, 0, 0), (b, ac, 0, 0), (c, ab, 0, 0), (ab, c, 0, 0), (ac, b, 0, 0), (bc, a, 0, 0), (0, a, bc, 0), (0, b, ac, 0), (0, c, ab, 0), (0, ab, c, 0), (0, ac, b, 0), (0, bc, a, 0), (0, a, b, c), (0, a, c, b), (0, b, a, c), (0, b, c, a), (0, c, a, b), (0, c, b, a), (a, 0, b, c), (a, 0, c, b), (b, 0, a, c), (b, 0, c, a), (c, 0, a, b), (c, 0, b, a), (a, b, 0, c), (a, c, 0, b), (b, c, 0, a), (b, a, 0, c), (c, a, 0, b), (c, b, 0, a), (a, b, c, 0), (a, c, b, 0), (b, a, c, 0), (b, c, a, 0), (c, a, b, 0), (c, b, a, 0)\} \quad (28)$$

where the superscripts, i.e., the x of Λ_{comb}^x , give the order of the sum, $i + j$. For example, for the first order case, since $i + j = a$, the possible combinations for the (i, j) pair in eq 23 can be $\{(0, a), (a, 0)\}$. Thus, eq 23 can be expanded as

$$\mathbf{S}^a = \sum_{(i,j) \in \Lambda_{\text{comb}}^a} \mathbf{C}^{i\dagger} \mathbf{s} \mathbf{C}^j = \mathbf{C}^{0\dagger} \mathbf{s} \mathbf{C}^a + \mathbf{C}^{a\dagger} \mathbf{s} \mathbf{C}^0$$

Similarly, for the second order case, the combinations for the (i, j) pair can be

$$\{(0, ab), (ab, 0), (a, b), (b, a)\}$$

and

$$\{(0, abc), (abc, 0), (a, bc), (b, ac), (c, ab), (ab, c), (ac, b), (bc, a)\}$$

for the third order case. This notation will be used throughout the rest of this work.

Applying eq 22 to eq 5, we can have the perturbation terms of the inverse matrix as

$$\mathbf{S}^{-1}(\vec{E}) = \mathbf{S}^{(0)-1} + E^a \mathbf{S}^{(a)-1} + (2!)^{-1} E^a E^b \mathbf{S}^{(ab)-1} + (3!)^{-1} E^a E^b E^c \mathbf{S}^{(abc)-1} + \dots \quad (29)$$

where $\mathbf{S}^{(0)-1}$ is given in eq 5 and $\mathbf{S}^{(a)-1}$, $\mathbf{S}^{(ab)-1}$, and $\mathbf{S}^{(abc)-1}$ are defined as

$$\mathbf{S}^{(a)-1} = -\mathbf{X} \mathbf{S}^a \mathbf{X} \quad (30)$$

$$\mathbf{S}^{(ab)-1} = -\mathbf{X} \mathbf{S}^{ab} \mathbf{X} \quad (31)$$

$$\mathbf{S}^{(abc)-1} = -\mathbf{X} \mathbf{S}^{abc} \mathbf{X} \quad (32)$$

Substituting eqs 19 and 29 into eq 10, which is the unperturbed density matrix, leads to the perturbed density matrices corresponding to different orders in eq 21:

$$\mathbf{D}^a = 2 \sum_{(i,j,k) \in \Lambda_{\text{comb}}^a} \mathbf{C}^i \mathbf{S}^{(j)-1} \mathbf{C}^{k\dagger} \quad (33)$$

$$\mathbf{D}^{ab} = 2 \sum_{(i,j,k) \in \Lambda_{\text{comb}}^{ab}} \mathbf{C}^i \mathbf{S}^{(j)-1} \mathbf{C}^{k\dagger} \quad (34)$$

$$\mathbf{D}^{abc} = 2 \sum_{(i,j,k) \in \Lambda_{\text{comb}}^{abc}} \mathbf{C}^i \mathbf{S}^{(j)-1} \mathbf{C}^{k\dagger} \quad (35)$$

Equation 20 shows the expansion of the Fock/Kohn–Sham matrix. The zero order of the expansion is already given in eq 12. Other orders are expressed as

$$\mathbf{F}^a = \mathbf{h}^a + \mathbf{V}_J^a + \mathbf{V}_{xc}^a \quad (36)$$

where the dipole moment matrix, \mathbf{h}^a ($a \in \{x, y, z\}$), is defined as

$$h_{st}^a = -\langle \chi_s | e \cdot \mathbf{a} | \chi_t \rangle$$

Since the dipole moment matrix has no terms higher than the first order, the second and third order expansions of the operator are

$$\mathbf{F}^{ab} = \mathbf{V}_J^{ab} + \mathbf{V}_{xc}^{ab} \quad (37)$$

$$\mathbf{F}^{abc} = \mathbf{V}_J^{abc} + \mathbf{V}_{xc}^{abc} \quad (38)$$

According to eqs 20 and 36–38, we define \mathbf{G} matrices as

$$\mathbf{G}^0 = \mathbf{C}^{0\dagger} \mathbf{F}^0 \mathbf{C}^0 \quad (39)$$

$$\mathbf{G}^a = \mathbf{C}^{0\dagger} \mathbf{F}^a \mathbf{C}^0 \quad (40)$$

$$\mathbf{G}^{ab} = \mathbf{C}^{0\dagger} \mathbf{F}^{ab} \mathbf{C}^0 \quad (41)$$

$$\mathbf{G}^{abc} = \mathbf{C}^{0\dagger} \mathbf{F}^{abc} \mathbf{C}^0 \quad (42)$$

Similar to the conventional method, we also introduce a transformation matrix, \mathbf{U} ,

$$\mathbf{C}^a = \mathbf{C}^0 \mathbf{U}^a \quad (43)$$

$$\mathbf{C}^{ab} = \mathbf{C}^0 \mathbf{U}^{ab} \quad (44)$$

$$\mathbf{C}^{abc} = \mathbf{C}^0 \mathbf{U}^{abc} \quad (45)$$

After we have obtained the NOLMO based density matrices for each order, the static polarizabilities and hyperpolarizabilities can be calculated as

$$\alpha_{ab} = -\text{Tr}[\mathbf{h}^a \mathbf{D}^b] \quad (46)$$

$$\beta_{abc} = -\text{Tr}[\mathbf{h}^a \mathbf{D}^{bc}] \quad (47)$$

$$\gamma_{abcd} = -\text{Tr}[\mathbf{h}^a \mathbf{D}^{bcd}] \quad (48)$$

which are the same as the conventional methods. A detailed derivation of eqs 46–48 can be found in ref 9. Then the challenge is how to calculate the density matrices for each order of eqs 33–35.

With a static external electric field, the energy of a NOLMO-SCF reference (eq 7) can also be expanded as

$$\Omega(\vec{E}) = \Omega^0 + E^a \Omega^a + (2!)^{-1} E^a E^b \Omega^{ab} + (3!)^{-1} E^a E^b E^c \Omega^{abc} + \dots \quad (49)$$

with Ω^0 the unperturbed ground state energy of the system (eq 7) while other energies corresponding to the perturbation orders are

$$\Omega^a = 2\text{Tr}(\sum_{(i,j,k,l) \in \Lambda_{\text{comb}}^a} \mathbf{C}^{i\dagger} \mathbf{F} \mathbf{C}^k \mathbf{S}^{(l)-1}) \quad (50)$$

$$\Omega^{ab} = 2\text{Tr}(\sum_{(i,j,k,l) \in \Lambda_{\text{comb}}^{ab}} \mathbf{C}^{i\dagger} \mathbf{F} \mathbf{C}^k \mathbf{S}^{(l)-1}) \quad (51)$$

$$\Omega^{abc} = 2\text{Tr}(\sum_{(i,j,k,l) \in \Lambda_{\text{comb}}^{abc}} \mathbf{C}^{i\dagger} \mathbf{F} \mathbf{C}^k \mathbf{S}^{(l)-1}) \quad (52)$$

The energy W of a molecular system perturbed by an external electric field \vec{E} is

$$\begin{aligned} W(\vec{E}) = W^0 - \mu_a E^a - (2!)^{-1} \alpha_{ab} E^a E^b - (3!)^{-1} \beta_{abc} E^a E^b E^c \\ - (4!)^{-1} \gamma_{abcd} E^a E^b E^c E^d + \dots \end{aligned} \quad (53)$$

where $\mu_a = -\text{Tr}[\mathbf{h}^a \mathbf{D}^0]$ is the a ($a \in \{x, y, z\}$) component of the dipole moment, and all other variables are defined as given previously. Comparing eq 49 with eq 53, we can build equations for solving the transformation matrix \mathbf{U} (eqs 43–45) corresponding to each perturbation order, which leads to the solution to eqs 33–35,

$$\sum_{(i,j,k,l) \in \Lambda_{\text{comb}}^a} \mathbf{C}^{i\dagger} \mathbf{F} \mathbf{C}^k \mathbf{S}^{(l)-1} = \frac{1}{2} \mathbf{h}^a \mathbf{D}^0 \quad (54)$$

Applying eqs 30, 39, 40, 43, and $\mathbf{S}^{(0)-1} = \mathbf{X}$ in eq 54, we reach a matrix equation for calculating the first order transformation matrix, \mathbf{U} , as

$$\mathbf{G}^0 \mathbf{X} \mathbf{U}^{a\dagger} - \mathbf{U}^{a\dagger} \mathbf{G}^0 \mathbf{X} = \mathbf{G}^a \mathbf{X} - \frac{1}{2} \mathbf{h}^a \mathbf{D}^0 \quad (55)$$

Similar operation results in the second order transformation matrix as

$$\mathbf{G}^0 \mathbf{X} \mathbf{U}^{ab\dagger} - \mathbf{U}^{ab\dagger} \mathbf{G}^0 \mathbf{X} = \mathbf{G}^{ab} \mathbf{X} - \frac{1}{2} \mathbf{h}^a \mathbf{D}^b + \mathbf{B} \quad (56)$$

where the matrix \mathbf{B} for the second order case is defined as

$$\begin{aligned} \mathbf{B} = (\mathbf{G}^0 \mathbf{U}^a + \mathbf{G}^a + \mathbf{U}^{a\dagger} \mathbf{G}^0) \mathbf{S}^{(b)-1} + (\mathbf{G}^0 \mathbf{U}^b + \mathbf{G}^b + \mathbf{U}^{b\dagger} \mathbf{G}^0) \mathbf{S}^{(a)-1} \\ + (\mathbf{G}^a \mathbf{U}^b + \mathbf{G}^b \mathbf{U}^a + \mathbf{U}^{a\dagger} \mathbf{G}^0 \mathbf{U}^b + \mathbf{U}^{b\dagger} \mathbf{G}^0 \mathbf{U}^a \\ - \mathbf{G}^0 \mathbf{X} (\mathbf{U}^{a\dagger} \mathbf{S}^0 \mathbf{U}^b + \mathbf{U}^{b\dagger} \mathbf{S}^0 \mathbf{U}^a)) \mathbf{X} \end{aligned} \quad (57)$$

which is obtained from the first order calculation and remains constant during the second order calculation. Finally the equation for the third order transformation matrix is

$$\mathbf{G}^0 \mathbf{X} \mathbf{U}^{abc\dagger} - \mathbf{U}^{abc\dagger} \mathbf{G}^0 \mathbf{X} = \mathbf{G}^{abc} \mathbf{X} - \frac{1}{2} \mathbf{h}^a \mathbf{D}^{bc} + \mathbf{T} \quad (58)$$

with the constant matrix \mathbf{T} defined as

$$\begin{aligned} \mathbf{T} = \sum_{i,j,k \in \{a,b,c\}} (\mathbf{G}^0 \mathbf{U}^i + \mathbf{G}^i + \mathbf{U}^{i\dagger} \mathbf{G}^0) \mathbf{S}^{(jk)-1} - \mathbf{G}^0 \mathbf{X} (\sum_{(i,j) \in \Lambda_{\text{comb}}^{abc}} \mathbf{U}^{i\dagger} \mathbf{S}^0 \mathbf{U}^j) \mathbf{X} \\ + \sum_{i,j,k \in \{a,b,c\}} \mathbf{U}^{i\dagger} (\mathbf{G}^0 \mathbf{U}^j + \mathbf{G}^j + \mathbf{G}^j \mathbf{U}^k + \mathbf{G}^k \mathbf{U}^j) \mathbf{X} \\ + \sum_{i,j,k \in \{a,b,c\}} [\mathbf{U}^{ij\dagger} (\mathbf{G}^0 \mathbf{U}^k + \mathbf{G}^k) + \mathbf{G}^k \mathbf{U}^{ij} + \mathbf{G}^j \mathbf{U}^k] \mathbf{X} \\ + \sum_{i,j,k \in \{a,b,c\}} (\mathbf{G}^0 \mathbf{U}^{ij} + \mathbf{G}^{ij} + \mathbf{U}^{ij\dagger} \mathbf{G}^0 + \mathbf{G}^i \mathbf{U}^j + \mathbf{G}^j \mathbf{U}^i + \mathbf{U}^{i\dagger} \mathbf{G}^0 \mathbf{U}^j \\ + \mathbf{U}^{j\dagger} \mathbf{G}^0 \mathbf{U}^i + \mathbf{U}^{i\dagger} \mathbf{G}^j + \mathbf{U}^{j\dagger} \mathbf{G}^i) \mathbf{S}^{(k)-1} \end{aligned} \quad (59)$$

where

$$\Lambda_{\text{comb}}^{abc} = \{(a,bc), (b,ac), (c,ab), (ab,c), (ac,b), (bc,a)\}$$

III. IMPLEMENTATION

The theory given earlier shows how to calculate the static polarizabilities and hyperpolarizabilities of a system with NOLMO. Since this is a novel method that is first developed, we have solved several difficulties during the implementation of the theory. In this section, we will describe the solutions to these difficulties.

1. Virtual Orbital Coefficients Generation. Our method is based on an unperturbed ground state NOLMO restricted reference.¹⁸ Although both the occupied orbitals and the virtual orbitals are generated from initial guess, the current NOLMO-SCF method mainly optimizes the occupied orbitals of the system and leaves the virtual orbitals unchanged. Therefore, in order to carry out the calculation described in section II, we need to generate the virtual orbital coefficients corresponding to the occupied orbitals of the ground state reference.

Since in our method the orthogonal condition of the orbitals has been removed, the obtained occupied orbitals are not orthogonal to each other. This nonorthogonality is also suitable for the virtual orbitals. However, we have to keep the occupied orbitals space orthogonal to the virtual orbitals space. Therefore, the virtual orbital coefficient generation becomes how to find the projection of the occupied orbitals at the null space:

$$\mathbf{C}^{\text{occ}\dagger} \mathbf{s} \mathbf{C}^{\text{vir}} = 0 \quad (60)$$

where \mathbf{C}^{occ} is the submatrix of the occupied orbitals part of the \mathbf{C} matrix obtained from the reference, \mathbf{s} is the AO overlap integral matrix defined previously, and \mathbf{C}^{vir} is the submatrix we would like to find out. Since both \mathbf{C}^{occ} and \mathbf{s} are given, we can define a coefficient matrix $\mathbf{A} = \mathbf{C}^{\text{occ}\dagger} \mathbf{s}$, and rewrite eq 60 as

$$\mathbf{A} \mathbf{C}^{\text{vir}} = 0 \quad (61)$$

To find out \mathbf{C}^{vir} , we need to find the null space projection of the \mathbf{A} matrix. The singular value decomposition (SVD) algorithm⁴⁸ was used to generate the projection. After the decomposition, the generated matrix \mathbf{V}^T of the SVD output contains the submatrix of \mathbf{C}^{vir} . In the present calculations, we could, but did not, carry out the localization within the subspace of the virtual orbitals. The localization of the virtual orbitals does not change any equation but will affect the efficiency for $O(N)$ calculations, which will be addressed in a future study.

2. Efficient Generation of the \mathbf{U} Matrix. The key step for solving each order of the CPSCF equation lies on the generation of the \mathbf{U} matrix in each iteration (eqs 56, 57, and 59). Conventionally, this kind of matrix equation is written as (taking the first order case as an example) $\mathbf{U}^a \varepsilon^0 - \varepsilon^0 \mathbf{U}^a = \mathbf{G}^a$, of which the off-diagonal block of the matrix \mathbf{U} (the diagonal blocks of \mathbf{U} are set to zero) can be solved as $\mathbf{U}_{ij}^a = \mathbf{G}_{ij}^a / (\varepsilon_j^0 - \varepsilon_i^0)$, because the coefficient matrix, ε^0 , is diagonal. However, in our method, because of the use of the noncanonical MO, the coefficient matrix will be no longer diagonal. Again, taking the first order case as example, the linear matrix equation (eq 56) is

$$\mathbf{G}^0 \mathbf{X} \mathbf{U}^{a\dagger} - \mathbf{U}^{a\dagger} \mathbf{G}^0 \mathbf{X} = \mathbf{G}^a \mathbf{X} - \frac{1}{2} \mathbf{h}^a \mathbf{D}^0$$

For simplicity, we set $\mathbf{A} = \mathbf{G}^0 \mathbf{X}$, $\mathbf{Y} = \mathbf{U}^{a\dagger}$ (for higher order cases, $\mathbf{Y} = \mathbf{U}^{ab\dagger}$ and $\mathbf{Y} = \mathbf{U}^{abc\dagger}$), and $\mathbf{Z} = \mathbf{G}^a \mathbf{X} - (1/2) \mathbf{h}^a \mathbf{D}^0$ ($\mathbf{Z} = \mathbf{G}^{ab} \mathbf{X} - (1/2) \mathbf{h}^a \mathbf{D}^b + \mathbf{B}$ and $\mathbf{Z} = \mathbf{G}^{abc} \mathbf{X} - (1/2) \mathbf{h}^a \mathbf{D}^{bc} + \mathbf{T}$ for

higher order cases). So a general form of eqs 56, 57, and 59 can be written as

$$AY - YA = Z \quad (62)$$

which is classified as a displacement equation, a special case of the well-known Sylvester equation.⁴⁹ The condition for such an equation to have a unique solution is that the Kronecker product,

$$K = I \otimes A - A^T \otimes I$$

is nonsingular, where I is a unit matrix of the same dimension as A . Otherwise the equation can have an infinite number of solutions or none. In our case, the Kronecker product is singular. Then the problem becomes how to solve this ill-conditioned linear matrix equation. There are many methods in the literature for solving this kind of equation.^{50–53} Here we mainly use the idea of the Tikhonov's regularization algorithm.⁵⁴ This algorithm introduces a regularization parameter, λ , to an ill-posed linear equation, $Ax = b$, of which the matrix A is ill-conditioned. To make a regular linear equation, one solves $(A - \lambda I)x = b$, without losing significant accuracy, with proper choice of λ . However, in our case, if we transform eq 62 into a linear equation via the Kronecker product,

$$Ky = z \quad (63)$$

where $y = \text{vec}(Y)$ and $z = \text{vec}(Z)$, the space complex for storing matrix K would be at the $O(N^4)$ level (if A is $N \times N$) and the time complex for solving such a linear equation (after regularization) will be roughly $O(N^6)$. This is not suitable for us if we want to develop a linear-scaling method. Inspired by the Tikhonov's regularization algorithm, we introduce a regularization parameter to eq 62,

$$AY - YA - \lambda IY = Z \quad (64)$$

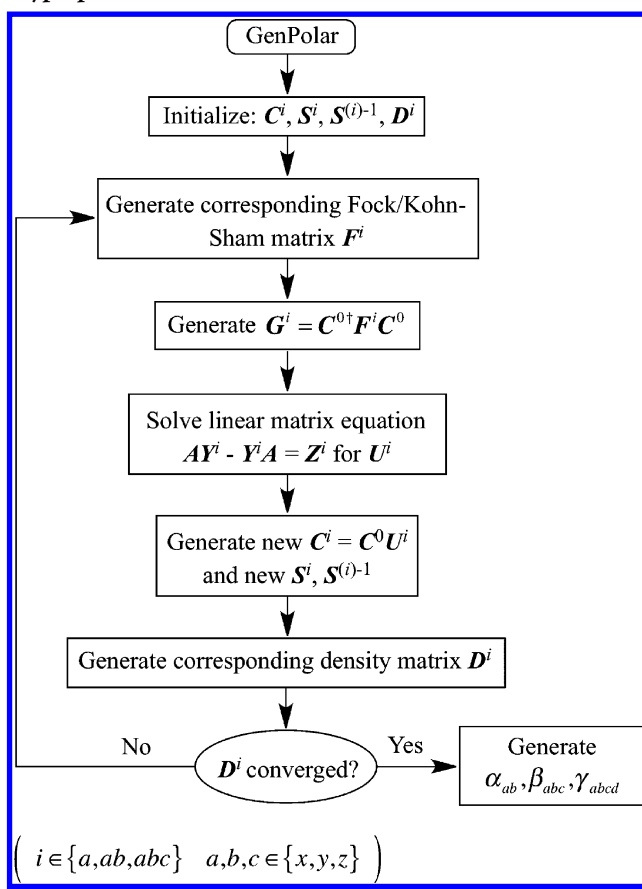
Further transforming eq 64 to $(A - \lambda I)Y - YA = Z$ and introducing $A' = A - \lambda I$, eq 64 can be rewritten as

$$A'Y - YA = Z \quad (65)$$

which is a typical Sylvester equation. There are many different efficient algorithms to solve such an equation,^{55,56} and we have mainly used the DGEES (for Schur decomposition of matrices A' and A) and DTRSIL (for back-substitution to solve Y) subroutines implemented in the LAPACK library.⁵⁷ However, in order to keep the result as accurate as possible, the regularization parameter in eq 64 should be small enough. According to Yang et al.,⁵³ the regularization gives good result when the parameter is set as 10^{-4} to 10^{-6} . However, in our case, we found that when it is set as 0.0012, the best accuracy can be achieved (see Discussion).

3. Iterative Solution to α_{ab} , β_{abc} , and γ_{abcd} . When calculating the static polarizabilities and hyperpolarizabilities, α_{ab} , β_{abc} , and γ_{abcd} , we start with zero initial orbital coefficient matrices, C^i ($i \in \{a, ab, abc\}$). Then the corresponding initial S^i , $S^{(i)-1}$, D^i , F^i , and G^i can be obtained. With these initial matrices, the matrix equation (eq 62) is solved to obtain the U^i matrices. Then new C^i , S^i , $S^{(i)-1}$, D^i , and F^i can be formed. The process is repeated until the density matrices have converged (Chart 1). Once the density matrices are converged, the polarizabilities and hyperpolarizabilities are calculated via eqs 46–48.

Chart 1. Iterative Process of Calculating Polarizabilities and Hyperpolarizabilities



IV. NUMERICAL TESTS OF THE METHOD

The present method has been implemented in the program developed in our group.¹⁸ We use GAMESS⁴⁶ for benchmark calculations. In order to verify our method, we have chosen several different types of molecular systems based on recent studies.^{58–60} The static polarizabilities and hyperpolarizabilities of water dimer, naphthalene, 1-fluorobenzene, and $\text{CH}_2(\text{CH})_8\text{CH}_2$ were calculated via both our method and the standard CPSCF method in the program package GAMESS under the same level of theory and the same basis sets. All calculations were carried out on a Xeon E5504 2.0 GHz CPU. And the basis sets we have used in our calculation were 3-21G, 4-31G, and 6-31G.

Before CPSCF calculations, the structures of the testing systems were optimized. We have used the Gaussian 09 program package⁶¹ to carry out the structure optimization at the DFT B3LYP level of theory^{62,63} with aug-cc-pvdz basis sets. The second derivatives of the energy for the systems were also calculated to ensure that the systems are at their global minimum. The optimized structure of the testing systems is given in Figure 1.

For CPSCF calculations, we have applied the same basis sets, i.e., 3-21G, 4-31G, and 6-31G, to both of our code and the reference GAMESS code. The calculated static polarizability and hyperpolarizabilities of the testing systems are given in Table 1. From Table 1 we can see that, for the chosen systems, the accuracy of our method can be always good enough. However, because we introduced a regularization parameter for

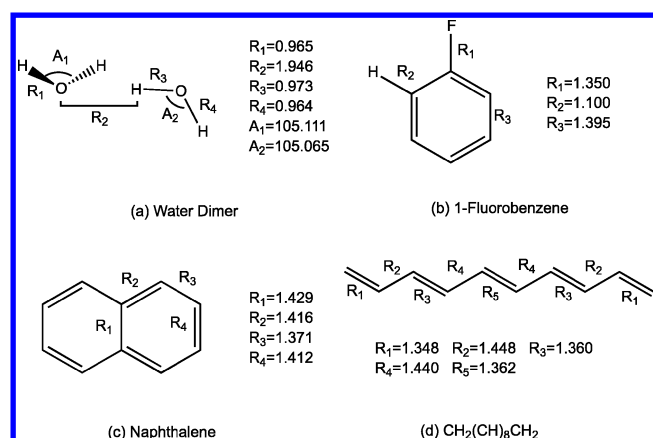


Figure 1. Ground state configuration of the systems used for demonstration. Based on ground states optimization with the DFT calculations, the optimized bond lengths of all of the test systems and the bond angles of the water dimer system are given (length units, Å).

solving eqs 56, 57, and 59, the accuracy can be monitored by varying the value of the parameter.

V. DISCUSSION

Compared with the benchmarking results, the testing results given in the previous section show that the accuracy of our method is promising. However, slight differences between the results of our method and those of the benchmark do exist. This mainly comes from two aspects: the accuracy of the NOLMO-SCF reference and the regularization parameter, λ in eq 64, we have chosen. Figure 2 shows us the relationship between the accuracy of the second order hyperpolarizabilities and various regularization parameters. The $\text{CH}_2(\text{CH})_8\text{CH}_2$ system has been used as an example. The parameter varies from 2.0×10^{-5} to 1.5×10^{-2} . Each parameter corresponds to a unique $\langle\gamma\rangle$. The differences between these $\langle\gamma\rangle$ and the reference $\langle\gamma\rangle$ were calculated. From Figure 2, we can see that there are actually two minima to achieve the best accuracy. However, with $\lambda = 1.2 \times 10^{-3}$, all of the systems we have chosen can achieve a good accuracy. But the other minimum ($\lambda = 1.235 \times 10^{-2}$) is only suitable for the $\text{CH}_2(\text{CH})_8\text{CH}_2$ system.

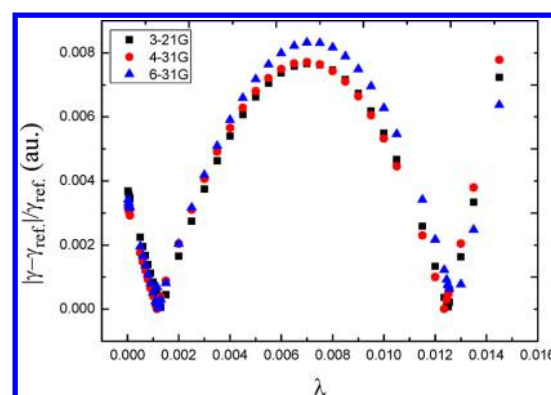


Figure 2. Relationship between the accuracy of our method and the regularization parameter we have chosen. The parameter varies from 2.0×10^{-5} to 1.5×10^{-2} .

Therefore, we have used $\lambda = 1.2 \times 10^{-3}$ as the regularization parameter in our implementation. This is also consistent with the preference of using a regularization parameter sufficient to remove the singularity but as small as possible to maintain accuracy.

Also, since NOLMO-CPSCF method expands the wave function and Fock/Kohn–Sham operator to different perturbation orders, the accuracy of the NOLMO-SCF reference will directly affect the accuracy of our method. By varying the energy convergence threshold of the NOLMO-SCF calculation, e.g., from 10^{-8} to 10^{-12} , we can see this effect clearly; i.e., the more accurate the reference is, the more accurate (hyper)polarizabilities can be obtained (Figure 3).

However, at this stage, we have mainly focused on the derivation of the underlying equations and provided the first tests to ensure the correctness of the proposed method. We could but have not considered the efficiency aspect during the development. All of the linear-scaling related techniques, e.g., the cutoff and the sparse matrix schemes and so on, are not applied in our current implementation. Nevertheless, our method can perform slightly better than the conventional method iteratively (Table 2). Since the γ calculation takes most of the elapsed time when computing the static polarizabilities

Table 1. Static Polarizability, First Hyperpolarizability, and Second Hyperpolarizability for the Testing Systems

test systems		basis sets					
		3-21G		4-31G		6-31G	
		NOLMO ^d	conv. ^e	NOLMO	conv.	NOLMO	conv.
water dimer	$\langle\alpha\rangle^a$	8.02	8.02	8.73	8.73	8.89	8.89
	β_{vec}^b	25.01	25.01	30.04	30.04	29.82	29.82
	$\langle\gamma\rangle^c$	156.4	156.3	213.0	212.7	218.9	218.6
1-fluoro-benzene	$\langle\alpha\rangle$	49.20	49.19	50.95	50.95	52.17	52.17
	β_{vec}	271.5	271.5	300.4	300.4	304.1	304.2
	$\langle\gamma\rangle$	449.8	447.7	568.8	565.6	591.1	587.1
naphthalene	$\langle\alpha\rangle$	88.98	88.98	91.57	91.57	93.58	93.57
	β_{vec}	0.00	0.00	0.00	0.00	0.00	0.00
	$\langle\gamma\rangle$	1.113(3) ^f	1.105(3)	1.305(3)	1.298(3)	1.344(3)	1.336(3)
$\text{CH}_2(\text{CH})_8\text{CH}_2$	$\langle\alpha\rangle$	161.3	161.3	164.9	164.9	167.8	167.8
	β_{vec}	0.00	0.00	0.00	0.00	0.00	0.00
	$\langle\gamma\rangle$	8.996(4)	8.993(4)	9.285(4)	9.286(4)	9.580(4)	9.580(4)

^a $\langle\alpha\rangle = (1/3) \sum_i \alpha_{ii}$ ($i \in \{x, y, z\}$; units, au). ^b $\beta_{\text{vec}} = (\sum_i \beta_i^2)^{1/2}$ with $\beta_i = (1/3) \sum_j (\beta_{ijj} + \beta_{jij} + \beta_{jji})$ ($i, j \in \{x, y, z\}$, at au). ^c $\langle\gamma\rangle = (1/15) \sum_{ij} (\gamma_{ijij} + \gamma_{jiij} + \gamma_{ijji})$ ($i, j \in \{x, y, z\}$; units, au). ^dNOLMO indicates our NOLMO based CPSCF code. ^eThe corresponding reference calculations of the GAMESS package. ^fNumbers in parentheses indicate the power of 10 by which the entry is to be multiplied.

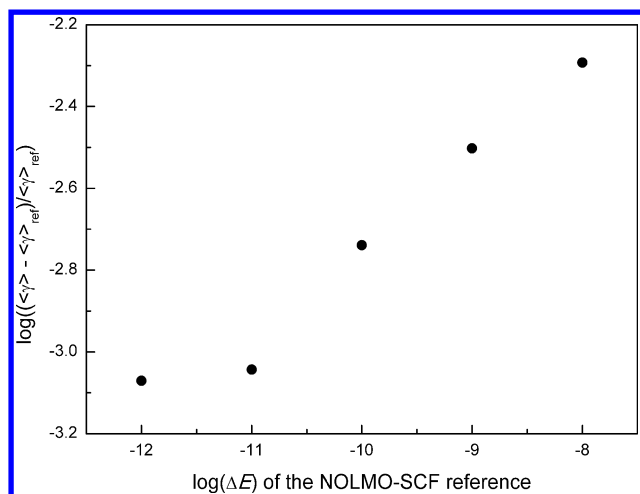


Figure 3. Relationship between the accuracy of our method and the accuracy of the NOLMO-SCF reference calculations.

and hyperpolarizabilities, Table 2 mainly uses the CPU wall time of γ generation to show the efficiency of our unaccelerated method. From Table 2 we can see that although, in general, our method performs slower than the conventional method because our method iterates more cycles than the conventional method, iteratively, our method slightly outperforms the conventional method. This is promising even for an unaccelerated method.

In future work, the linear-scaling related technologies, e.g., the cutoff scheme, sparse matrix technique, and quick Fock/KS matrix generation technique, etc., will be employed in our method. Moreover, we plan to include frequency dependence into our current equations to develop a NOLMO based TDSCF method. To make the method linear scaling, a divide-and-conquer style^{64,65} scheme will also be introduced in our future NOLMO-TDSCF implementation.

VI. SUMMARY

In this work we have reformulated CPSCF equations based on NOLMO. In an AO basis, and starting from a NOLMO-SCF reference, the wave function and SCF operator are expanded to different orders of the static electric field. The equations up to the third order have been derived. Because of the release of orthogonal restrictions on MOs, the derived equations are very different from those of a conventional method based on canonical MOs. These equations have been implemented into our computer program. Water dimer, benzene, 1-fluorobenzene, and $\text{CH}_2(\text{CH})_8\text{CH}_2$ have been used to verify the method. The results demonstrated the accuracy of our method. This work represents the first step toward efficient calculations of molecular response and excitation properties with NOLMOs.

AUTHOR INFORMATION

Corresponding Author

*E-mail: gu@scnu.edu.cn.

Notes

The authors declare no competing financial interest.

ACKNOWLEDGMENTS

We thank the China Postdoctoral Science Foundation (Grant 2013M531863) and the National Natural Science Foundation of China (Grants 21273081 and 21073067) for financial support. F.L.G. is grateful to the Project Supported by Guangdong Province Universities and Colleges Pearl River Scholar Funded Scheme.

REFERENCES

- (1) *Nonlinear optical properties of organic molecules and crystals*; Chemla, D. S., Zyss, J., Eds.; Academic Press: San Diego, CA, USA, 1987.
- (2) *Introduction to Nonlinear Optical Effects in Molecules and Polymers*; Prasad, P. N., Williams, D. J., Eds.; Wiley: New York, 1991.
- (3) Coe, B. J.; Harris, J. A.; Jones, L. A.; Brunschwig, B. S.; Song, K.; Clays, K.; Garin, J.; Orduna, J.; Coles, S. J.; Hursthouse, M. B. *J. Am. Chem. Soc.* **2005**, *127*, 4845–4859.
- (4) Terenziani, F.; Katan, C.; Badaeva, E.; Tretiak, S.; Blanchard-Desce, M. *Adv. Mater.* **2008**, *20*, 4641–4678.
- (5) Baba, M.; Kowaka, Y.; Nagashima, U.; Ishimoto, T.; Goto, H.; Nakayama, N. *J. Chem. Phys.* **2011**, *135*, No. 054305.
- (6) Castet, F.; Rodriguez, V.; Pozzo, J. L.; Ducasse, L.; Plaquet, A.; Champagne, B. *Acc. Chem. Res.* **2013**, *46*, 2656–2665.
- (7) Olsen, J.; Jorgensen, P. *J. Chem. Phys.* **1985**, *82*, 3235–3264.
- (8) Sekino, H.; Bartlett, R. J. *J. Chem. Phys.* **1986**, *85*, 3945–3949.
- (9) Karna, S. P.; Dupuis, M. *J. Comput. Chem.* **1991**, *12*, 487–504.
- (10) Weiss, H.; Ahlrichs, R.; Haser, M. *J. Chem. Phys.* **1993**, *99*, 1262–1270.
- (11) Christiansen, O.; Jorgensen, P.; Hattig, C. *Int. J. Quantum Chem.* **1998**, *68*, 1–52.
- (12) Gauss, J. Molecular Properties. In *Modern Methods and Algorithms of Quantum Chemistry Proceedings*, NIC Series, 2nd ed.; Grotendorst, J., Ed.; John von Neumann Institute for Computing: Jülich, Germany, 2000; Vol. 3, pp 541–592.
- (13) Furche, F. *J. Chem. Phys.* **2001**, *114*, 5982–5992.
- (14) Salek, P.; Vahtras, O.; Helgaker, T.; Agren, H. *J. Chem. Phys.* **2002**, *117*, 9630–9645.
- (15) Wang, F.; Yam, C. Y.; Chen, G. *J. Chem. Phys.* **2007**, *126*, No. 244102.
- (16) Pople, J. A.; Krishnan, R.; Schlegel, H. B.; Binkley, J. S. *Int. J. Quantum Chem.* **1979**, *16*, 225–241.
- (17) Kussmann, J.; Beer, M.; Ochsenfeld, C. *WIREs Comput. Mol. Sci.* **2013**, *3*, 614–636.
- (18) Peng, L.; Gu, F. L.; Yang, W. T. *Phys. Chem. Chem. Phys.* **2013**, *15*, 15518–15527.

Table 2. CPU Wall Clock Time Analysis of Our Method Compared with the Conventional Method^a

	timing analysis of γ generation (with 6-31G basis sets; unit, s)							
	water dimer		1-fluorobenzene		naphthalene		$\text{CH}_2(\text{CH})_8\text{CH}_2$	
	NOLMO	conv.	NOLMO	conv.	NOLMO	conv.	NOLMO	conv.
γ overall	0.55	0.34	25.78	14.84	199.41	94.06	88.67	60.52
total iteration of γ	239	148	310	174	419	191	377	251
CPU time per iteration	0.00230	0.00230	0.0832	0.0853	0.476	0.492	0.235	0.241

^aWe have used the CPU timing data of the γ calculation as an example because this calculation takes most of the CPU time when generating the static polarizabilities and hyperpolarizabilities. The total number of iterations for computing γ of the two methods has been given. And the CPU time for each iteration has been listed in italics.

- (19) Zuehlsdorff, T. J.; Hine, N. D. M.; Spencer, J. S.; Harrison, N. M.; Riley, D. J.; Haynes, P. D. *J. Chem. Phys.* **2013**, *139*, No. 064104.
- (20) White, C. A.; Head-Gordon, M. *J. Chem. Phys.* **1994**, *101*, 6593–6605.
- (21) White, C. A.; Johnson, B. G.; Gill, P. M. W.; Head-Gordon, M. *Chem. Phys. Lett.* **1994**, *230*, 8–16.
- (22) Gustavson, F. G. *ACM Trans. Math. Softw.* **1978**, *4*, 250–269.
- (23) Korchowiec, J.; Gu, F. L.; Imamura, A.; Kirtman, B.; Aoki, Y. *Int. J. Quantum Chem.* **2005**, *102*, 785–794.
- (24) Boys, S. F. *Rev. Mod. Phys.* **1960**, *32*, 296–299.
- (25) von Niessen, W. *J. Chem. Phys.* **1972**, *56*, 4290–4297.
- (26) Pipek, J.; Mezey, P. G. *J. Chem. Phys.* **1989**, *90*, 4916–4926.
- (27) Cioslowski, J. *Int. J. Quantum Chem.* **1990**, *37*, 291–307.
- (28) Bytautas, L.; Ruedenberg, K. *Mol. Phys.* **2002**, *100*, 757–781.
- (29) Weber, V.; Hutter, J. *J. Chem. Phys.* **2008**, *128*, No. 064107.
- (30) Kirtman, B.; Dykstra, C. E. *J. Chem. Phys.* **1986**, *85*, 2791–2796.
- (31) Kirtman, B.; DeMelo, C. P. *J. Chem. Phys.* **1987**, *86*, 1624–1631.
- (32) Imamura, A.; Aoki, Y.; Maekawa, K. *J. Chem. Phys.* **1991**, *95*, 5419–5431.
- (33) Aoki, Y.; Gu, F. L. *Prog. Chem.* **2012**, *24*, 886–909.
- (34) Aoki, Y.; Gu, F. L. *Phys. Chem. Chem. Phys.* **2012**, *14*, 7640–7668.
- (35) Yokojima, S.; Chen, G. H. *Chem. Phys. Lett.* **1999**, *300*, 540–544.
- (36) Chen, G. H.; Yokojima, S.; Liang, W. Z.; Wang, X. J. *Pure Appl. Chem.* **2000**, *72*, 281–291.
- (37) Yoshikawa, T.; Kobayashi, M.; Fujii, A.; Nakai, H. *J. Phys. Chem. B* **2013**, *117*, 5565–5573.
- (38) O’Leary, B.; Duke, B. J.; Eilers, J. E. Utilization of Transferability in Molecular Orbital Theory. In *Advances in Quantum Chemistry*, Per-Olov, L., Ed.; Academic Press: New York, 1975; Vol. 9, pp 1–67.
- (39) Feng, H. S.; Bian, J.; Li, L. M.; Yang, W. T. *J. Chem. Phys.* **2004**, *120*, 9458–9466.
- (40) Burger, S. K.; Yang, W. T. *J. Phys.: Condens. Matter* **2008**, *20*, No. 294209.
- (41) Cui, G. L.; Fang, W. H.; Yang, W. T. *Phys. Chem. Chem. Phys.* **2010**, *12*, 416–421.
- (42) Cui, G.; Fang, W.; Yang, W. *J. Phys. Chem. A* **2010**, *114*, 8878–8883.
- (43) Reboredo, F. A.; Williamson, A. J. *Phys. Rev. B* **2005**, *71*, No. 121105.
- (44) Kussmann, J.; Ochsenfeld, C. *J. Chem. Phys.* **2007**, *127*, No. 204103.
- (45) Ding, F.; Van Kuiken, B. E.; Eichinger, B. E.; Li, X. *J. Chem. Phys.* **2013**, *138*, No. 064104.
- (46) Schmidt, M. W.; Baldridge, K. K.; Boatz, J. A.; Elbert, S. T.; Gordon, M. S.; Jensen, J. H.; Koseki, S.; Matsunaga, N.; Nguyen, K. A.; Su, S.; Windus, T. L.; Dupuis, M.; Montgomery, J. A., Jr. *J. Comput. Chem.* **1993**, *14*, 1347–1363.
- (47) Yang, W. T. *Phys. Rev. B* **1997**, *56*, 9294–9297.
- (48) *Numerical Recipes: The Art of Scientific Computing*, 3rd ed.; Press, W. H., Teukolsky, S. A., Vetterling, W. T., Flannery, B. P., Eds.; Cambridge University Press: New York, 2007; pp 65–75.
- (49) Sylvester, J. J. *Acad. Sci., Paris, C. R.* **1884**, *99* (67–71), 115–116.
- (50) Wu, Q.; Yang, W. T. *J. Theor. Comput. Chem.* **2003**, *2*, 627–638.
- (51) Deng, L. J.; Huang, T. Z.; Zhao, X. L.; Zhao, L.; Wang, S. *J. Opt. Soc. Am. A* **2013**, *30*, 948–955.
- (52) Mantilla-Gaviria, I. A.; Leonardi, M.; Balbastre-Tejedor, J. V.; de los Reyes, E. *Math. Comput. Modell.* **2013**, *57*, 1999–2008.
- (53) Heaton-Burgess, T.; Bulat, F. A.; Yang, W. *Phys. Rev. Lett.* **2007**, *98*, No. 256401.
- (54) Franklin, J. N. *Math. Comput.* **1974**, *28*, 889–907.
- (55) Bartel, R. H.; Stewart, G. W. *Commun. ACM* **1972**, *15*, 820–826.
- (56) Golub, G. H.; Nash, S.; Van Loan, C. *IEEE Trans. Autom. Control* **1979**, *AC-24*, 909–913.
- (57) Gutheil, I. Basic Numerical Libraries for Parallel Systems. In *Modern Methods and Algorithms of Quantum Chemistry Proceedings*, NIC Series, 2nd ed.; Grotendorst, J., Ed.; John von Neumann Institute for Computing: Jülich, Germany, 2000; Vol. 3, pp 47–65.
- (58) Karna, S. P. *Chem. Phys. Lett.* **1993**, *214*, 186–192.
- (59) Balu, R.; Korambath, P.; Pandey, R.; Karna, S. P. *Chem. Phys. Lett.* **2013**, *590*, 58–62.
- (60) Alparone, A. *Comput. Theor. Chem.* **2013**, *1013*, 23–24.
- (61) Frisch, M. J.; Trucks, G. W.; Schlegel, H. B.; Scuseria, G. E.; Robb, M. A.; Cheeseman, J. R.; Scalmani, G.; Barone, V.; Mennucci, B.; Petersson, G. A.; Nakatsuji, H.; Caricato, M.; Li, X.; Hratchian, H. P.; Izmaylov, A. F.; Bloino, J.; Zheng, G.; Sonnenberg, J. L.; Hada, M.; Ehara, M.; Toyota, K.; Fukuda, R.; Hasegawa, J.; Ishida, M.; Nakajima, T.; Honda, Y.; Kitao, O.; Nakai, H.; Vreven, T.; Montgomery, J. A., Jr.; Peralta, J. E.; Ogliaro, F.; Bearpark, M.; Heyd, J. J.; Brothers, E.; Kudin, K. N.; Staroverov, V. N.; Keith, T.; Kobayashi, R.; Normand, J.; Raghavachari, K.; Rendell, A.; Burant, J. C.; Iyengar, S. S.; Tomasi, J.; Cossi, M.; Rega, N.; Millam, J. M.; Klene, M.; Knox, J. E.; Cross, J. B.; Bakken, V.; Adamo, C.; Jaramillo, J.; Gomperts, R.; Stratmann, R. E.; Yazyev, O.; Austin, A. J.; Cammi, R.; Pomelli, C.; Ochterski, J. W.; Martin, R. L.; Morokuma, K.; Zakrzewski, V. G.; Voth, G. A.; Salvador, P.; Dannenberg, J. J.; Dapprich, S.; Daniels, A. D.; Farkas, O.; Foresman, J. B.; Ortiz, J. V.; Cioslowski, J.; Fox, D. J. *Gaussian 09*, Revision D.01; Gaussian: Wallingford, CT, USA, 2013.
- (62) Lee, C.; Yang, W.; Parr, R. G. *Phys. Rev. B* **1988**, *37*, 785–789.
- (63) Becke, A. D. *J. Chem. Phys.* **1993**, *98*, 1372–1377.
- (64) Yang, W. *Phys. Rev. Lett.* **1991**, *66*, 1438–1441.
- (65) Yang, W. T.; Lee, T. S. *J. Chem. Phys.* **1995**, *103*, 5674–5678.